

A MOLECULAR HYPER-MESSAGE PASSING NETWORK WITH FUNCTIONAL GROUP INFORMATION

Fangying Chen*, Junyoung Park*, Jinkyoo Park
KAIST

Daejeon, Korea

{gyjin32, junyoungpark, jinkyoo.park}@kaist.ac.kr

ABSTRACT

We proposed the molecular hyper-message passing network (MolHMPN) that predicts the properties of a molecule with prior knowledge-guided subgraph. Modeling higher-order connectivities in molecules is necessary as changes in both the pair-wise and higher-order interactions among atoms results in the change of molecular properties. Many approaches have attempted to model the higher-order connectivities. However, those methods relied heavily on data-driven approaches, and it is difficult to determine if the utilized subgraphs contain any properties of interest or have any significance on the molecular properties. Hence, we propose MolHMPN to utilize the functional group prior knowledge and model the pair-wise and higher-order connectivities among the atoms in a molecule. Molecules can contain many types of functional groups, which affect the properties the molecules. For example, the toxicity of a molecule is associated with toxicophores, such as nitroaromatic groups and thiourea. MolHMPN uses functional groups to construct hypergraphs, modifies the hypergraph using domain knowledge-guided modification scheme, embeds the graph and hypergraph inputs using a hypergraph message passing (HyperMP) layer, and uses the updated graph and hypergraph embeddings to predict the properties of the molecules. Our model provides a way to utilize prior knowledge in chemistry for molecular properties prediction tasks, and balance between the usage of prior knowledge and data-driven modification adaptively. We show that our model is able to outperform the other baseline methods for most of the dataset, and show that using domain knowledge-guided data-learning is effective.

1 Introduction

Toxicological screening is vital for the development of new drugs, the evaluation of the therapeutic potential of existing molecules, and the assessment of pharmacological activity and toxicity potential of new molecules on human. Traditionally, toxicity studies of molecules relied on animal testing, which can provide inadequate bases for predicting clinical outcomes on humans [1]. The U.S. Food and Drug Administration (FDA) has also estimated that it takes more than eight years to test and study a new drug before its approval to the general public, which includes early laboratory and animal testing [9]. Machine learning (ML) methods have therefore been utilized widely to assess the effects that chemicals have on humans and the environment as it is able to utilize data with large data sizes, while reducing the time and cost it takes for drugs approval, and avoiding costly late-stage failures.

In ML, graph neural networks (GNNs) have been used actively in molecule-related tasks for their ability to represent molecules as graphs. Representing molecules as graphs is natural and preferred since the molecular structure is inextricably linked to the molecular properties. In the graphs, the atoms and bonds of the molecules are represented by the nodes and edges of the graphs. These methods take the graphs as inputs and use the node features to predict the molecular properties. The connectivities between the nodes in the graphs include the pair-wise connectivities between two nodes that are connected by an edge, and the higher-order connectivities between nodes that are further apart.

To model the pair-wise connectivities in the graphs, the message passing neural network (MPNN) [11], which is a representative GNN architecture, has been devised as a fast simulation method to replace computationally expensive quantum mechanical simulations. Its variants [35, 29] have also shown their potentials in molecular properties prediction tasks. These pair-wise methods can model higher-order connectivities by stacking multiple MPNN layers. This, however,

can cause the model to suffer from oversmoothing [27] or oversquashing [2] problems. Alternatively, the higher-order connectivities can be modeled by augmenting substructures, such as introducing virtual nodes [19] or combining multiple nodes [30, 17, 14]. Similarly, hypergraphs contain hyperedges that are made up of nodes from a subgraph [8, 4]. Examples of such subgraphs include frequently-occurring substructures [17], K-hop neighbor substructures [14], and residual substructures that are unspecified by the graph adjacency matrix [19]. However, these methods have focused exclusively on data-driven approaches and it is hard to determine if those subgraphs contain any properties of interest or have any significance on the molecular properties.

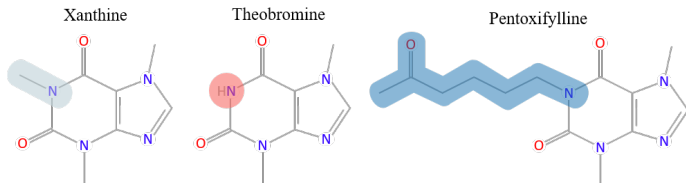


Figure 1: Molecules of similar structures but different properties. Xanthine is found in caffeine and temporarily prevents or reduces drowsiness, theobromine is found in cacao and has mood improving effect, and pentoxifylline is a drug used to treat muscle pain in people with peripheral artery disease. The colored parts show their difference. The grey and red parts show that the pair-wise interactions between two atoms can change the properties of the molecules, and the grey/red and blue parts show that the higher-order interactions between atoms can change molecular properties.

In chemistry, molecules are constructed from a carbon skeleton, onto which functional groups are attached to. The carbon skeleton is a chain of carbon atoms and is relatively unreactive. On the other hand, functional group is a group of atoms that are bonded together in a particular fashion, and determines the properties of the molecules (e.g. solubility, reactivity and lipophilicity) [6]. Figure 1 shows examples of molecules that have similar structures but with different properties. From Figure 1, the difference in the number of methyl, amine and ketone groups has resulted in the different effects that the compounds have on the human body [18]; the changes in the pair-wise and higher-order interactions among the atoms can change the properties of the molecules. Hence, accounting for both pair-wise and higher-order interactions among atoms is essential for molecular properties prediction. The current study aims to incorporate the prior knowledge of functional groups to model the higher-order interactions in the molecule to ensure that the subgraphs are significant to the molecular properties of the molecules. The incorporation of prior knowledge to neural networks (NNs) has been attempted by several methods for their specific tasks [26, 25, 21, 36]. However, it is difficult to determine which prior knowledge to exploit in closed form for the learning pipelines, and the wrong selection of prior knowledge can deteriorate the performances of the learning models. Therefore, ML models that can leverage the prior knowledge *partially* and overcome the potentially unsuitable prior knowledge are needed.

In this paper, we propose a molecular hyper-message passing network (MoLHMPN) that is able to predict the properties of a molecule with prior knowledge-guided substructures. Our model (MoLHMPN) predicts the molecular properties by conducting the following sequential operations:

- **Constructing hypergraphs using functional groups.** Given a graph representation of a molecule that is constructed from its simplified molecular-input line-entry system (SMILES) string, MoLHMPN constructs the hyperedges according to functional groups that have been identified by chemists to represent the higher-order connectivities among the atoms. Each hyperedge represents a functional group that is present in a molecule. The hyperedges can also be extended up to their K -hop neighborhood.
- **Embedding the graph and hypergraph using hypergraph message passing layer (HyperMP).** The HyperMP consists of an atom graph convolution (AtomGC) and a functional group graph convolution (FuncGC) for the graphs and hypergraphs respectively. It performs message passing on the graphs and hypergraphs sequentially.
- **Modifying the hypergraph using the computed embeddings.** MoLHMPN modifies the input hypergraph by considering the original graph and hypergraph, and their respective embedded representations. This process updates the prior knowledge (i.e., input hypergraphs) with observations (i.e., embeddings) similar to that of the Bayesian approaches.
- **Predicting the molecular properties from the modified hypergraph.** MoLHMPN applies HyperMP again to compute the embedding with the original graph and modified hypergraph, and predict the target label with the updated embeddings.

The key contribution of the current study is on the adaptation of functional groups using prior knowledge and the utilization of the prior knowledge selectively when conducting the molecular prediction tasks. Our novelties are summarized as follows:

- **Providing a way to utilize the prior knowledge.** MolHMPN translates functional groups, which are based upon prior knowledge in chemistry, into hyperedges to process higher-order connectivities in molecules effectively.
- **Balancing between prior knowledge and data-driven scheme.** Without heavily relying on the functional group prior knowledge, MolHMPN modifies such information adaptively depending on the target input. This can alleviate risk of using unsuitable information or representations of the target molecule.

We evaluate the effectiveness of MolHMPN on several datasets that are used for molecular properties classification and regression tasks, and show that MolHMPN is able to outperform the other baseline methods for most datasets. We also analyze the usage of different types of substructures and the effectiveness of the prior knowledge-guided data-driven modification for the prediction tasks.

2 Methodology

This section highlights the methodology of the proposed MolHMPN. In MolHMPN, the hypergraphs are first constructed using the prior knowledge of functional groups and extended up to their K -hop neighborhood. The graph and constructed hypergraphs are then embedded using the HyperMP layer(s) so as to modify the membership of the hyperedges using the computed embeddings. The graph and modified hypergraphs are then embedded again using the HyperMP layer(s) to predict the target label with the updated embedding. Figure 2 shows the overall architecture of MolHMPN.

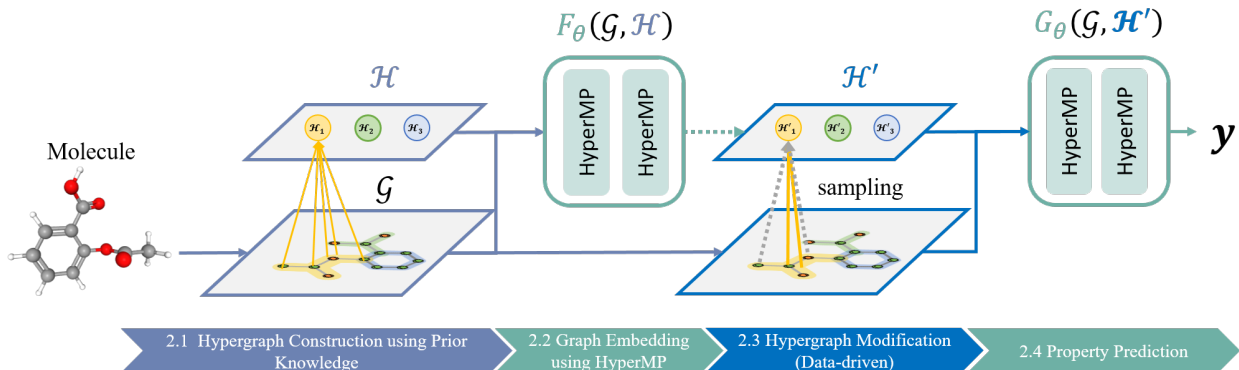


Figure 2: Overall architecture of MolHMPN

2.1 Hypergraph construction

Inspired by the significance of functional groups on the molecular properties as discussed in section 1, we utilize the knowledge of functional groups that are defined by chemists to let the model identify the similarities and differences of the molecules more easily. We represent the molecules as conventional pair-wise graphs and hypergraphs. The conventional pair-wise graphs are defined as $\mathcal{G} = \{\mathbb{V}, \mathbb{E}\}$, where $\mathbb{V} = \{v_1, \dots, v_n\}$ is a set of n nodes (atoms), and $\mathbb{E} \subset \mathbb{V} \times \mathbb{V}$ is a set of edges (bonds). The edge e_{ij} exists if a bond between v_i and v_j exists. The features of v_i and e_{ij} are defined as x_i and x_{ij} respectively. The hypergraph is defined as $\mathcal{H} = \{\mathcal{H}_k | k = 1, \dots, n_K\}$, where \mathcal{H}_k is k^{th} hyperedge that has a set of nodes as its members. The features of \mathcal{H}_k are defined as z_k .

When constructing \mathcal{H} , atoms in cyclic and acyclic (open-chain) groups are considered separately. The minimal collection of cycles in the molecules are extracted as \mathcal{H}_k . For the acyclic groups, the vicinity of the functional group is considered when extracting the hyperedge representation, which is defined as the central atom and the atoms that are attached to it [18]. The main atoms that are used are carbon (C), nitrogen (N), oxygen (O), phosphorus (P) and sulfur (S), and the main bond types that are used are the single ($-$), double ($=$) and triple bonds (\equiv). The extraction process of the acyclic groups can be described as follows:

1. Find a central atom (e.g., C, N, O, P or S) from \mathcal{G} and set it as v_c .
2. Find the 1-hop neighborhood set $\mathbb{F}_1(v_c)$ of v_c , which is given as $\mathbb{F}_1(v_c) = \{v_j \in \mathcal{N}(v_c) | t(v_j) \in \mathbb{A}_t, t(e_{ij}) \in \mathbb{B}_t\}$, where $\mathcal{N}(v_c)$ is the neighborhood of v_c , $t(\cdot)$ denotes the types of atom/bond, and $\mathbb{A}_t, \mathbb{B}_t$ are the sets of target atom and bond respectively that are based accordingly to the target functional group.
3. Find the 2-hop neighborhood set $\mathbb{F}_2(v_c)$ of v_c , which is given as $\mathbb{F}_2(v_c) = \{v_k \in \bigcup_{v_j \in \mathcal{N}(v_i)} \mathcal{N}(v_j) | t(v_j) \neq \text{C} \vee t(e_{ij}) \neq -\}$.

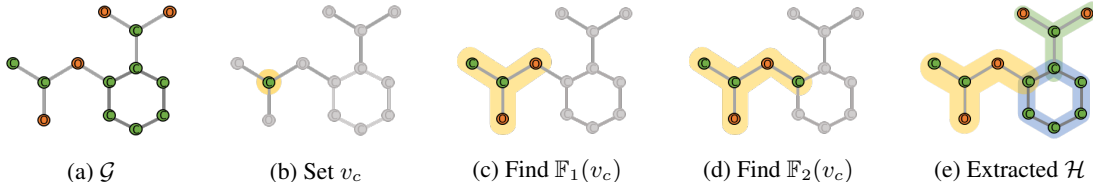


Figure 3: **Hypergraph construction for aspirin.** a) \mathcal{G} of aspirin. b) Set carbon as v_c . c) To find $\mathbb{F}_1(v_c)$, set $v_c - \text{O}$, $v_c = \text{O}$ and $v_c - \text{C}$, where $\{\text{O}, \text{C} \in \mathbb{A}_t\}$ and $\{-, = \in \mathbb{B}_t\}$. d) To find $\mathbb{F}_2(v_c)$, find v_j that is not C and e_{ij} that is not a single bond. e) All the extracted \mathcal{H}_k of \mathcal{G} .

4. The extracted hyperedge is hence $\mathcal{H}_k = \{v_c\} \cup \mathbb{F}_1(v_c) \cup \mathbb{F}_2(v_c)$.

Different combinations of the central atoms, and $\mathbb{A}_t, \mathbb{B}_t$ are used to match each functional group. Here, the prior knowledge of functional groups is applied in \mathbb{A}_t and \mathbb{B}_t . The remaining atoms that do not belong to any of the specified functional groups are put into the same hyperedge if they are connected by an edge. The 1-hop and 2-hop neighborhood sets are defined as changes in atom types within this range gives different functional groups. Figure A.1 shows an example of the hyperedge construction for the carboxyl group in aspirin. The list of functional groups used in this paper are given in Appendix A.1.

As we want to let the model leverage the prior knowledge (i.e. functional group) *partially* and overcome potentially unsuitable prior knowledge, we consider an extension of the hyperedges so that a much higher-order interaction can be captured by the hyperedges. In that regard, the hyperedges are extended up to their K -local neighborhood as follows:

$$\mathcal{H}_k = \bigcup_{v_i \in \mathcal{H}_k} \mathcal{N}_K(v_i) \quad (1)$$

where $\mathcal{N}_K(v_i)$ is the K -hop neighborhood set of v_i . This extension allows the hyperedge modification in Section 2.3 to be guided by the prior knowledge while being restricted to the scope of the hyperedge in the extended \mathcal{H}_k . \mathcal{G} and \mathcal{H} will then be fed into the HyperMP layer to compute the embedding that are needed to adjust the members of \mathcal{H}_k .

2.2 Graph and hypergraph embedding with Hypergraph message passing

Modeling both the pair-wise (atom/bond) and higher-order (functional group) connectivities is crucial for conducting the molecule property predictions. Hence, we introduce the hypergraph message passing HyperMP layer to integrate the information from both the atoms and functional groups. HyperMP updates the input graphs via two steps: atom graph convolution (AtomGC) and functional group graph convolution (FuncGC). The general equation of the HyperMP can be defined as:

$$\mathcal{G}', \mathcal{H}' = \text{HyperMP}(\mathcal{G}, \mathcal{H}) \quad (2)$$

where \mathcal{G}' and \mathcal{H}' are the updated graph and hypergraph respectively.

AtomGC. AtomGC is designed to model the pair-wise interactions between atoms that are bonded together. It involves updating the edge features using the features of the edges and nodes that it connects, and updating the node features using the updated edge features. The edge update step is given as:

$$x'_{ij} = f_{\text{bond}}(x_i, x_j, x_{ij}) \quad (3)$$

where x'_{ij} is the updated edge feature and $f_{\text{bond}}(\cdot)$ is the edge multi-layer perceptron (MLP). It is noteworthy that, for the target tasks, the edge information is essential as the chemical bonds contains crucial information about the molecular properties. In the node update step, the updated node features x'_i is computed with x'_{ij} as follows:

$$\alpha_{ij} = f_{\text{attn}}(x_i, x_j, x_{ij}) \quad (4)$$

$$x'_i = f_{\text{atom}}\left(x_i, \sum_{j \in \mathcal{N}(i)} \alpha_{ij} x'_{ij}\right) \quad (5)$$

where α_{ij} is the attention coefficient of e_{ij} , $f_{\text{attn}}(\cdot)$ is the attention multi-layer perceptron (MLP) whose output activation is the sigmoid activation function, and $f_{\text{atom}}(\cdot)$ is the node MLP and $\mathcal{N}(i)$ is the neighborhood set of v_i . Here, unlike many attention modules that normalizes the attention scores so that the summation of the scores becomes 1.0, we normalize each attention score to be between 0.0 and 1.0. We empirically confirmed that this selection results in better prediction performance than the conventional attention scheme.

FuncGC. FuncGC is designed to model the higher-order interactions that are defined by the chemically-valid functional groups. Although the same functional groups can be present in many molecules, the effects that they have on the molecular properties may differ depending on their neighboring functional groups (or atoms). To account for such differences, we utilize the updated node feature that contains local information from the molecular graphs when generating the localized functional group features. We start the FuncGC by updating z_k using x'_i as follows:

$$\tilde{z}_k = g_{\text{atom} \rightarrow \text{fg}}\left(z_k, \sum_{i \in \mathcal{H}_k} x'_i\right) \quad (6)$$

where \tilde{z}_k is the localized feature that receives localized information from AtomGC, and $g_{\text{atom} \rightarrow \text{fg}}(\cdot)$ is the localizing MLP. Unlike \mathcal{G} , \mathcal{H} has no naturally defined edges as the functional groups are concepts rather than physically exist. Hence, the edges among the hyperedges are learnt as follows:

$$z'_{km} = g_{\text{edge}}(\tilde{z}_k, \tilde{z}_m) \quad (7)$$

where z'_{km} is the learnt edge feature between \mathcal{H}_k and \mathcal{H}_m , and g_{edge} is the edge MLP. z'_{km} thus captures the interaction between \mathcal{H}_k and \mathcal{H}_m . Lastly, the updated hyperedge features z'_k is computed with z'_{km} as follows:

$$\beta_{km} = g_{\text{attn}}(\tilde{z}_k, \tilde{z}_m) \quad (8)$$

$$z'_k = g_{\text{fg}}\left(z_k, \sum_{m \in \mathcal{H}} \beta_{km} z'_{km}\right) \quad (9)$$

where β_{km} is the attention coefficient between the k^{th} and the m^{th} hyperedge, $g_{\text{attn}}(\cdot)$ is the attention MLP whose output activation is sigmoid activation function as in AtomGC, and $g_{\text{fg}}(\cdot)$ is the hyperedge update function. The HyperMP layer is then used to modify the membership of the hyperedges and predict the molecular properties of the molecules using their respective computed embeddings.

Note that we did not design a path that propagate z'_k back to the members (atoms) of \mathcal{H}_k . This design works similar to the uninterrupted gradient path of LSTM [13] or the latent arrays of Perciever models [15]. We also experimentally confirmed that this design shows better prediction results.

2.3 Modifying the prior knowledge-guided structures

\mathcal{H} is constructed using the functional groups of the molecules. However, it is difficult to determine which prior knowledge to exploit in practice, and the wrong selection of prior knowledge can deteriorate the performances of the model. Hence, we allow models to adjust the members of \mathcal{H}_k , which is built upon the prior knowledge of functional groups, while predicting the molecular property. The general equation of the membership adjustment function $F_\theta(\mathcal{G}, \mathcal{H})$ can be defined as:

$$F_\theta(\mathcal{G}, \mathcal{H}) = \tilde{\mathcal{H}} \quad (10)$$

where $\tilde{\mathcal{H}}$ is the membership-adjusted hypergraph. It first uses the membership encoder $f_\theta(\cdot)$ to produce the membership-encoded features as follows:

$$\{\hat{x}_i\}, \{\hat{z}_k\} = f_\theta(\mathcal{G}, \mathcal{H}) \quad (11)$$

where \hat{x}_i and \hat{z}_k are the membership-encoded node and hyperedge features respectively, and $f_\theta(\cdot)$ is a stack of the HyperMP layer(s). As the memberships can be interpreted as a virtual "edge" between an atom v_i and its functional group \mathcal{H}_k , we employ a graph structure learning method to modify the membership. In the adjustment procedure, we consider the random discrete methods (i.e., the adjusted memberships are binary) which share a common philosophy with the Bayesian approaches. The membership adjustment procedure then starts by using the membership-encoded features to produce $\tilde{\mathcal{H}}$ as follows:

$$m_{ik} = g_\theta(\hat{x}_i, \hat{z}_k) \quad \forall v_i \in \mathcal{H}_k \quad (12)$$

$$\tilde{m}_{ik} = \text{sigmoid}\left(\left(\log\left(\frac{m_{ik}}{1 - m_{ik}}\right) + \epsilon_0 - \epsilon_1\right)/s\right) \quad \forall v_i \in \mathcal{H}_k \quad (13)$$

where m_{ik} is the bernoulli parameter that models the probability of the event that v_i becomes a member of \mathcal{H}_k , \tilde{m}_{ik} is the sampled membership, $g_\theta(\cdot)$ is the MLP whose output activation is the sigmoid function, ϵ_0 and ϵ_1 are the samples of Gumbel(0,1), and $s > 0$ is the temperature parameter. This procedure reparameterize the Bernoulli distribution via Gumbel reparameterization such that the (sampled) binary \tilde{m}_{ik} are differentiable [16]. By annealing $s \rightarrow 0$, we can recover $\tilde{m}_{ik} \sim \text{Ber}(m_{ik})$. We define the k^{th} adjusted hyperedge $\tilde{\mathcal{H}}_k = \{v_i \in \mathcal{H}_k \mid \tilde{m}_{ik} = 1\}$. $\tilde{\mathcal{H}}$ will then be used to produce the final predictions.

A similar approach is investigated in the context of pair-wise graph structure learning [28], where they assume that the edges of a complete graph is subjective to edge learning. On the other hand, we utilize this idea only to the members of hyperedges so as to provide a balance between the usage of prior knowledge and the data-driven scheme.

2.4 Molecular properties prediction

From the aforementioned methods, \mathcal{H} is first constructed using the prior knowledge of the functional groups from a given \mathcal{G} . The memberships of \mathcal{H} are then adjusted using $F_\theta(\mathcal{G}, \mathcal{H})$ to produce $\tilde{\mathcal{H}}$. Hence, in the final step of Mo1HMPN, the target label y of a given molecule is predicted by updating \mathcal{G} and $\tilde{\mathcal{H}}$ using the HyperMP layer as follows:

$$y = G_\theta(\mathcal{G}, \tilde{\mathcal{H}}) \quad (14)$$

where $G_\theta(\cdot)$ is the property prediction function, which consists of a stack of the HyperMP layer(s), a readout function, and a MLP.

2.5 Training model

For our tasks, we randomly split the datasets into 80:10:10 ratio as the training, validation and test sets and take the average of the results from different 5 random seeds (0 to 4). The atom and bond features that are used as the initial node and edge features are given in Appendix A.2. For $F_\theta(\cdot)$ and $G_\theta(\cdot)$, we use only one HyperMP layer each. The attentive sum and max function are used as the readout function of $G_\theta(\cdot)$. The loss functions for the classification and regression tasks are the binary cross-entropy (BCE) and mean squared error (MSE), respectively. We give extra weights to the minority class in the loss functions for the classification datasets based on the ratio of the minority to majority class of each task to handle the class imbalance problems. We train Mo1HMPN by minimizing the loss functions. We use the AdamP optimizer [12], whose learning rate is initialized as 0.001 and scheduled by the cosine annealing method [22]. We train the models for 500 epochs with mini-batch size of 512. More training details can be found in Appendix A.2. The results at the end of the training are recorded.

3 Results and discussion

In this section, we evaluate the performance of Mo1HMPN with several experiments. We first evaluate the performance of Mo1HMPN with several baseline methods that consider the pair-wise and/or high-order interactions in the molecules in Section 3.1. We then perform various ablation studies and show that it is beneficial to:

- **Section 3.2:** account for both the pair-wise and higher-order connectivities.
- **Section 3.3:** incorporate functional group information as the means of constructing hyperedge.
- **Section 3.4:** leverage the prior knowledge *partially* with the extended hyperedges.

The datasets that are used for evaluation includes Tox21, ClinTox, SIDER, BBBP, BACE, ESOL, FreeSolv and Lipophilicity. The detailed dataset description can be found in Appendix A.2. We provide the benchmark results and visualizations of Mo1HMPN to evaluate the performances.

3.1 Comparing with baseline models

We evaluate the performance of Mo1HMPN with baselines that make use of the pair-wise connectivities (*PAIR*) and/or higher-order connectivities (*HIGH*) in the molecules. For the *PAIR* baselines, we consider models using atoms only (MPNN (atom only)) [35], atom and bonds (MPNN) [35], directed bonds (DMPNN) [35], and atoms and bonds with enhanced interactions (CMPNN) [29]. For the *HIGH* baselines, we compare with baselines that have used substructures whose nodes are not connected by an edge (AGCN) [19], substructures with marginal nodes (GAAN) [30], and substructures that are constructed by junction tree (ML-MPNN) [33]. The results of the baselines are taken directly from their respective papers, except for CMPNN¹.

Table 1 shows the overall results of Mo1HMPN on graph classification and regression tasks. From the results, we can see that Mo1HMPN outperforms the other baselines for four out of eight datasets. From the *PAIR* results, we can see that the usage of atoms, undirected and directed bond information do not have a significant impact on the performances. Instead, increasing the interactions between the atoms and bonds (CMPNN) gives better results, especially for BBBP, ESOL and FreeSolv. Comparing Mo1HMPN with the *PAIR* models, we can see that the inclusion of higher-order connectivities is indeed beneficial for the tasks as Mo1HMPN outperforms the models for five out of eight datasets. Although the *PAIR* models can capture higher-order connectivities by using multiple layers, Mo1HMPN has outperformed the baselines with only one HyperMP layer as shown in Figure 4. From the *HIGH* results, we can see that Mo1HMPN outperforms the other baselines for three out of six datasets. Compared to the other *HIGH* models, ML-MPNN is the most similar to Mo1HMPN

¹We rerun their codes for all datasets as a mistake was found in their results as stated in their official code <https://github.com/SY575/CMPNN.git>

Table 1: **Benchmark results.** Comparing between different methods for molecular properties prediction. All results are taken from the original papers except CMPNN. Results in red are the best-performing results, and the results in blue are the second best-performing results. (\uparrow means that higher result is better and \downarrow means that lower result is better.)

Metric	Dataset	AUROC (Classification)					RMSE (Regression)		
		Tox21 (\uparrow)	ClinTox (\uparrow)	SIDER (\uparrow)	BBBP (\uparrow)	BACE (\uparrow)	ESOL (\downarrow)	FreeSolv (\downarrow)	Lipophilicity (\downarrow)
<i>PAIR</i>	● MPNN (atom only)	0.845	0.896	0.644	0.908	0.864	0.719	1.243	0.625
	★ MPNN	0.844	0.881	0.641	0.910	0.850	0.702	1.242	0.645
	✕ DMPNN	0.845	0.894	0.646	0.913	0.878	0.665	1.167	0.596
	▲ CMPNN	0.854	0.908	0.656	0.958	0.887	0.567	0.901	0.582
<i>HIGH</i>	● AGCN	0.802	0.868	0.592	—	—	0.306	1.33	0.736
	★ GAAN	0.839	0.888	0.658	—	—	0.294	1.057	0.605
	✕ ML-MPNN	0.852	0.892	0.689	—	—	0.571	1.052	0.560
	● MolHMPN	0.840	0.919	0.617	0.940	0.892	0.390	0.813	0.514

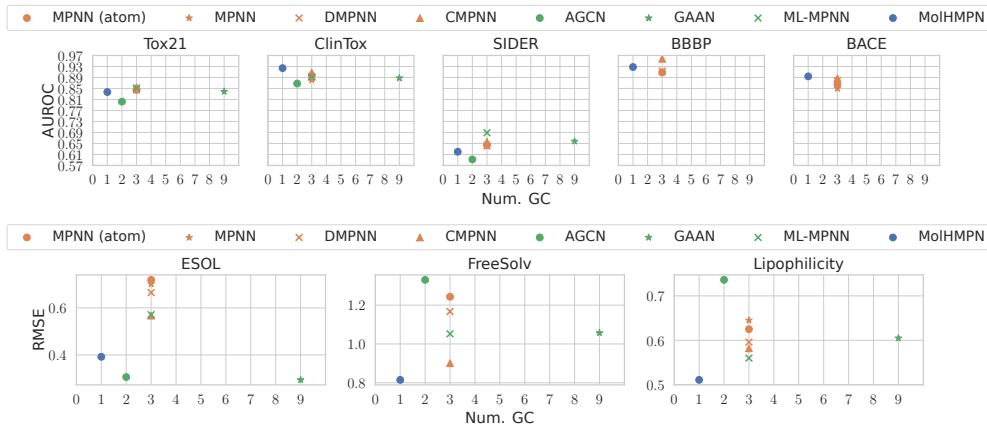


Figure 4: Number of graph convolutions vs. classification performances

as it integrates information from the nodes, edges, subgraphs and graphs, while MolHMPN integrates information from the nodes, edges and subgraphs. However, MolHMPN has outperformed ML-MPNN for four out of six datasets. This shows the efficacy of employing prior knowledge-guided hyperedges when conducting the benchmark tasks. Overall, the results shows the efficacy of accounting for both the pair-wise and higher-order connectivities, and employing prior knowledge-guided hyperedges.

Figure 5 shows the t-distributed stochastic neighbor embedding (t-SNE) plots of MolHMPN for all of the datasets, except for Tox21 and SIDER since it is not straightforward to define the toxicity or druglikeness of the molecules from the data labels. The classifications for ClinTox, BACE and BBBP are straightforward since they have less than 3 binary classification tasks. For the ESOL dataset, the molecules are considered to be druglike if their $\log P$ value is between -0.4 to 5.6 [10]. For FreeSolv, the molecules are considered to be druglike if their hydration free energy is below 0 kcal/mol, 0 to 1 kcal/mol for maybe druglike, and more than 1 kcal/mol for others [37]. For Lipophilicity, the molecules are considered to be druglike if their $\log D_{7.4}$ is above 0 [3]. The t-SNE plots will be analyzed in detail in the ablation studies.

3.2 Contribution of the pair-wise and higher-order connectivities

In Section 1, we made the hypothesis that both the pair-wise and higher-order connectivities should be accounted for in molecular properties predictions when we compare the structure of xanthine, theobromine and pentoxifylline. In the HyperMP layer, AtomGC accounts for the pair-wise connectivities while FuncGC accounts for the higher-order connectivities. Hence, to test this hypothesis, we devise the following variants:

- AtomGC: the entire FuncGC in the HyperMP layer is removed. Only the updated node features in the HyperMP layer are used for prediction.
- FuncGC: the entire AtomGC in the HyperMP layer is removed (i.e. the hyperedge features are no longer localized by the node features as in Equation 6. The localized features in Equations 6, 7 and 8 are the mean of the features of the nodes that are in the hyperedges). Only updated hyperedge features in the HyperMP layer are used for prediction.

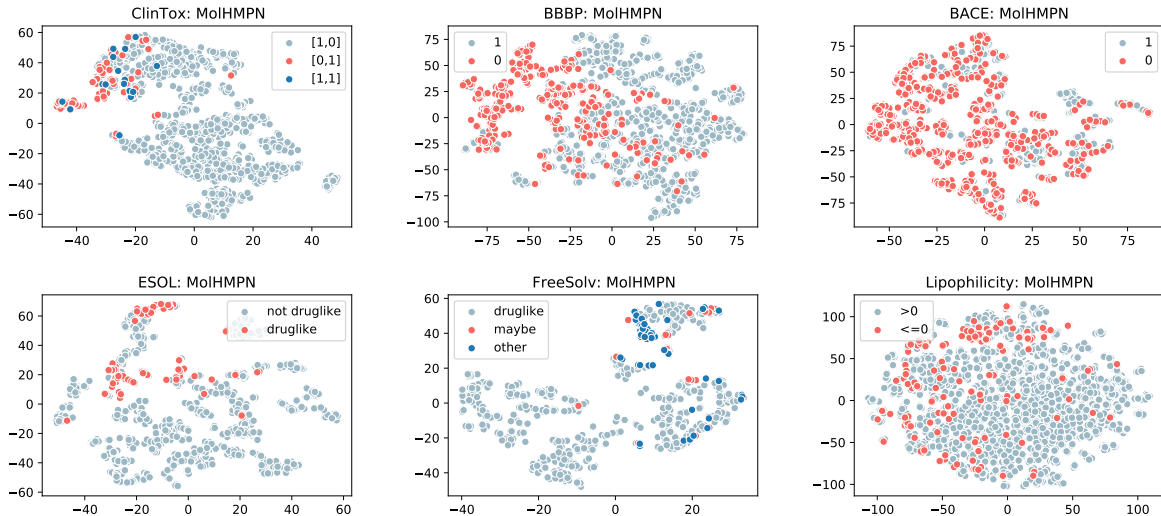


Figure 5: MolHMPN t-SNE plots

- MolHMPN-NoMod: MolHMPN with the original functional group design; the hyperedge extension and modification schemes are not implemented.

We evaluate the benchmark results and t-SNE plots of these variants. Note that the evaluation is done mainly for AtomGC, FuncGC and MolHMPN-NoMod since we are focusing on the analysis of the the pair-wise and higher-order connectivities contribution to the prediction performance, and not the hyperedge extension and modification in this section.

Table 2: **Design analysis.** Comparison between AtomGC, FuncGC and MolHMPN-NoMod. Results in bold are the best-performing results. (\uparrow means that higher result is better and \downarrow means that lower result is better.)

Metric	AUROC					RMSE		
Dataset	Tox21 (\uparrow)	ClinTox (\uparrow)	SIDER (\uparrow)	BBBP (\uparrow)	BACE (\uparrow)	ESOL (\downarrow)	FreeSolv (\downarrow)	Lipophilicity (\downarrow)
AtomGC	0.832 (± 0.0175)	0.897 (± 0.0390)	0.606 (± 0.001575)	0.901 (± 0.0197)	0.869 (± 0.0269)	0.436 (± 0.0552)	1.007 (± 0.3689)	0.561 (± 0.0786)
FuncGC	0.818 (± 0.0122)	0.830 (± 0.05641)	0.584 (± 0.0307)	0.887 (± 0.0303)	0.822 (± 0.0173)	0.668 (± 0.1163)	1.678 (± 0.6344)	0.782 (± 0.0502)
MolHMPN-NoMod	0.839 (± 0.0147)	0.909 (± 0.0394)	0.605 (± 0.0227)	0.928 (± 0.0302)	0.892 (± 0.0232)	0.447 (± 0.0559)	0.813 (± 0.3952)	0.517 (± 0.0415)

Table 2 shows the results of AtomGC, FuncGC and MolHMPN-NoMod. From Table 2, we can see that MolHMPN-NoMod outperforms the other models for six out of eight of the datasets, and more significantly for FreeSolv. We conjecture that this is because FreeSolv contain fragment-like compounds where the typical size of the molecules is substantially smaller than typical small-molecule drugs [24]. This makes the molecules more similar to the hyperedge design and hence, contributing significantly to the performance of MolHMPN-NoMod to FreeSolv. Among the three models, we can see that FuncGC performs the worst. This may be because there is no naturally defined edges between each hyperedge since two hyperedges may have more than one of the same node, making it difficult to design an edge that can define the relationship between two hyperedge well. Nonetheless, this does not mean that the incorporation of the functional group information degrades the performance of the model. This can be verified by comparing the results of AtomGC and MolHMPN-NoMod. From the results, we can see that the incorporation of functional group information has increased the performance of MolHMPN-NoMod as it has outperformed AtomGC for six out of eight datasets. This shows that using both the pair-wise and higher-order connectivities information is beneficial to the performances. We further verify this by visualizing the distribution of readout values of each model via t-SNE.

Figure 6 shows the t-SNE plot for the datasets. From the BACE and Lipophilicity plots, no clear separation can be observed. From the ESOL plots, it can be seen that AtomGC and MolHMPN-NoMod has similar data separation, which is consistent with the results in Table 2. From the ClinTox, BBBP and FreeSolv plots, a clearer separation can be seen as the minority plots are closer to each other with the incorporation of both the atom and functional group information, which is also consistent with the results in Table 2 and our hypothesis that both the pair-wise (atom) and higher-order

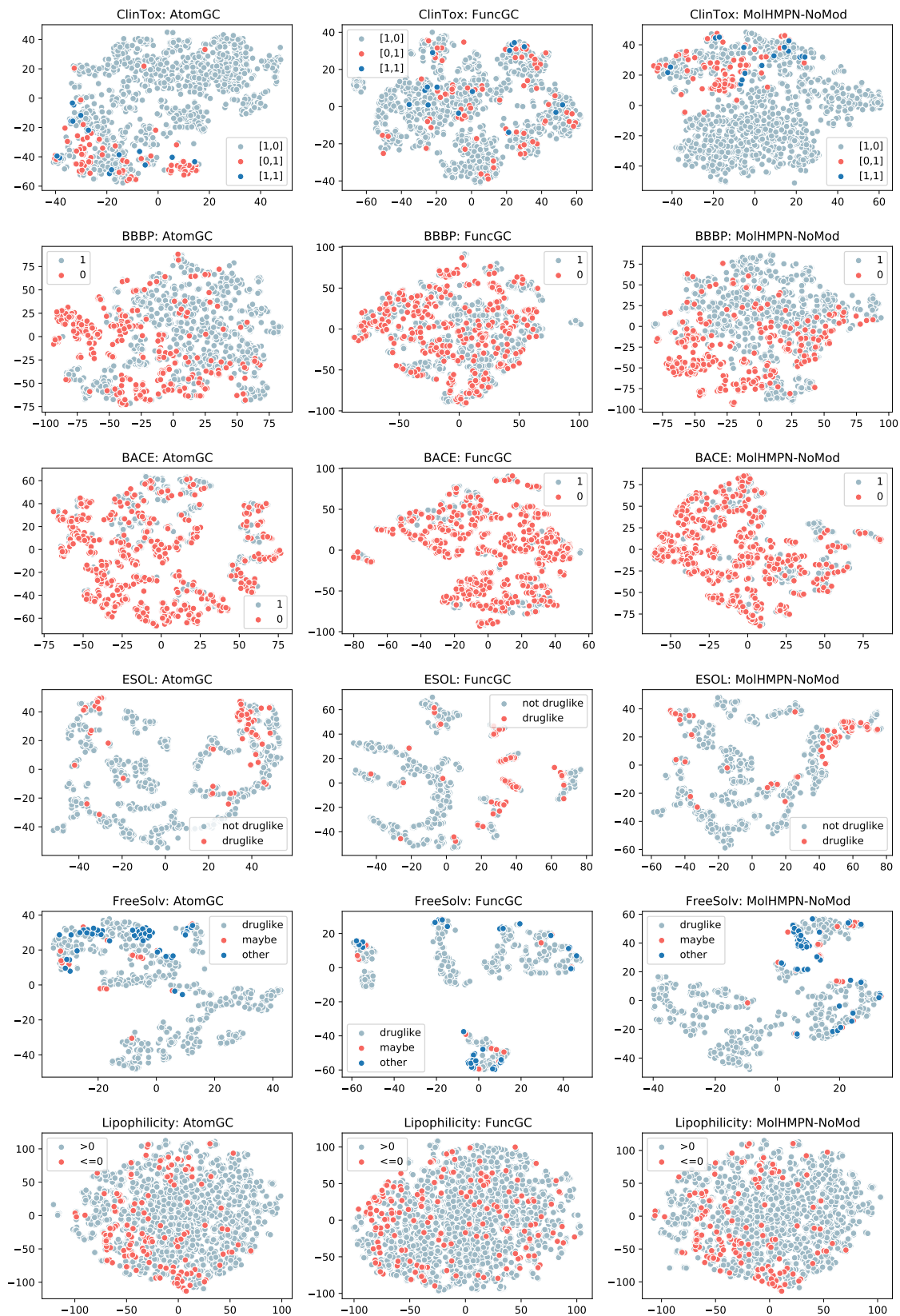


Figure 6: t-SNE plots for AtomGC, FuncGC and MolHMPN-NoMod. Analyzing the contributions of pair-wise and/or higher-order connectivities in MolHMPN

connectivities (functional groups) are important in molecular properties prediction tasks. This supports the benchmark results in Table 2 that integrating both the pair-wise and higher-order connectivities information is beneficial.

Overall, from the results in Table 2 and the visualizations in Figure 6, we can verify that incorporating both the pair-wise and higher-order connectivity information is beneficial to the performance of the model.

3.3 Comparison with different subgraphs

In Section 1, we made the hypothesis that substructures that are significant to the molecular properties should be used, and described the effects that functional groups have on the molecules. To test this hypothesis, we compare the performance of MolHMPN with other methods that employ other kinds of subgraphs and are known to be effective in solving molecule generation and graph meta-learning tasks. Since we are only analyzing the effectiveness of functional groups in molecular properties prediction tasks, we use the results of MolHMPN-NoMod. The subgraphs evaluated include:

- **Ring & Chemical Bond**: utilizes the set of ring structures and chemical bonds as the subgraph² [17]
- **K-hop neighbors**: utilizes the K-hop neighbors as subgraphs [14]
- **MolSoft**: utilizes the attention mechanism [32] to construct *soft* subgraphs. Refer to Appendix A.2 for more details.

1-hop neighbor is an edge-centric reformulation of the original graph where each hyperedge contains two nodes that are connected together by an edge, and MolSoft is approach that does not depend on prior knowledge and attempts to capture substructures that have significant effects to the molecular properties. Hence, the subgraphs that does not necessarily depend on the prior knowledge in chemistry (**Ring & Chemical Bond** and **K-hop neighbors**) and subgraphs that does not depend on prior knowledge (**MolSoft**) are evaluated to measure the significance of functional group to molecular properties prediction.

In the experiments, we replace the hyperedge construction rules with those of the baseline methods, and assess their performances with our benchmark datasets. Other than the hyperedge construction method, we use the same model and experiment setups as in Appendix A.2 to make fair comparisons.

Table 3: **Subgraph Comparison.** Comparison between different types of subgraphs. Results in red are the best-performing results, and the results in blue are the second best-performing results. (\uparrow means that higher result is better and \downarrow means that lower result is better.)

Metric	AUROC					RMSE		
Dataset	Tox21 (\uparrow)	ClinTox (\uparrow)	SIDER (\uparrow)	BBBP (\uparrow)	BACE (\uparrow)	ESOL (\downarrow)	FreeSolv (\downarrow)	Lipophilicity (\downarrow)
Ring & C. Bond	0.834 (± 0.0142)	0.911 (± 0.0401)	0.577 (± 0.0339)	0.919 (± 0.0124)	0.884 (± 0.0106)	0.477 (± 0.0547)	1.468 (± 0.5970)	0.520 (± 0.0475)
1-hop ngh.	0.833 (± 0.0194)	0.895 (± 0.0273)	0.597 (± 0.0246)	0.906 (± 0.0195)	0.869 (± 0.0297)	0.453 (± 0.0588)	1.128 (± 0.3030)	0.542 (± 0.1068)
2-hop ngh.	0.836 (± 0.0135)	0.910 (± 0.0448)	0.582 (± 0.0271)	0.926 (± 0.0314)	0.894 (± 0.0240)	0.431 (± 0.0709)	0.995 (± 0.3844)	0.564 (± 0.0475)
3-hop ngh.	0.830 (± 0.0147)	0.881 (± 0.0363)	0.597 (± 0.0307)	0.918 (± 0.0278)	0.871 (± 0.0136)	0.480 (± 0.1032)	1.078 (± 0.3094)	0.571 (± 0.0889)
MolSoft	0.803 (± 0.0161)	0.915 (± 0.0352)	0.588 (± 0.0300)	0.888 (± 0.0210)	0.871 (± 0.0311)	0.420 (± 0.0653)	1.049 (± 0.4940)	0.519 (± 0.0535)
MolHMPN-NoMod	0.839 (± 0.0147)	0.909 (± 0.0394)	0.605 (± 0.0227)	0.928 (± 0.0302)	0.892 (± 0.0232)	0.447 (± 0.0559)	0.813 (± 0.3952)	0.517 (± 0.0415)

Table 3 shows the results where different types of subgraphs are used. From Table 3, MolHMPN-NoMod has outperformed the other methods for five out of eight datasets, especially for FreeSolv. For SIDER, MolHMPN-NoMod has outperformed the other methods and has the smallest standard deviation. For BBBP, although 2-hop neighbor is comparable with MolHMPN-NoMod, MolHMPN-NoMod has a smaller standard deviation. One notable trend is that the 1-hop and 3-hop neighbor underperform as compared to 2-hop neighbor even though they model pair-wise and higher-order connectivities respectively. However, this is not observed in MolHMPN-NoMod even though we also employ up to 3-hop neighbors for the functional groups as subgraphs. This shows that, rather than increasing the size of the hyperedges, it is more important to select and specify which nodes to put in each hyperedge. For MolSoft, even though it performs well for ClinTox, ESOL and Lipophilicity, it did not perform as well for the rest of the datasets. Hence, from the results, we can verify that it is beneficial to employ prior knowledge (in our case, functional groups) to capture substructures that have significant effects on the molecular properties.

²In original paper, the frequently-occurring chemical subgraphs are also considered. However, in our benchmark datasets, none of the dataset satisfies the proposed value for occurrence frequency.

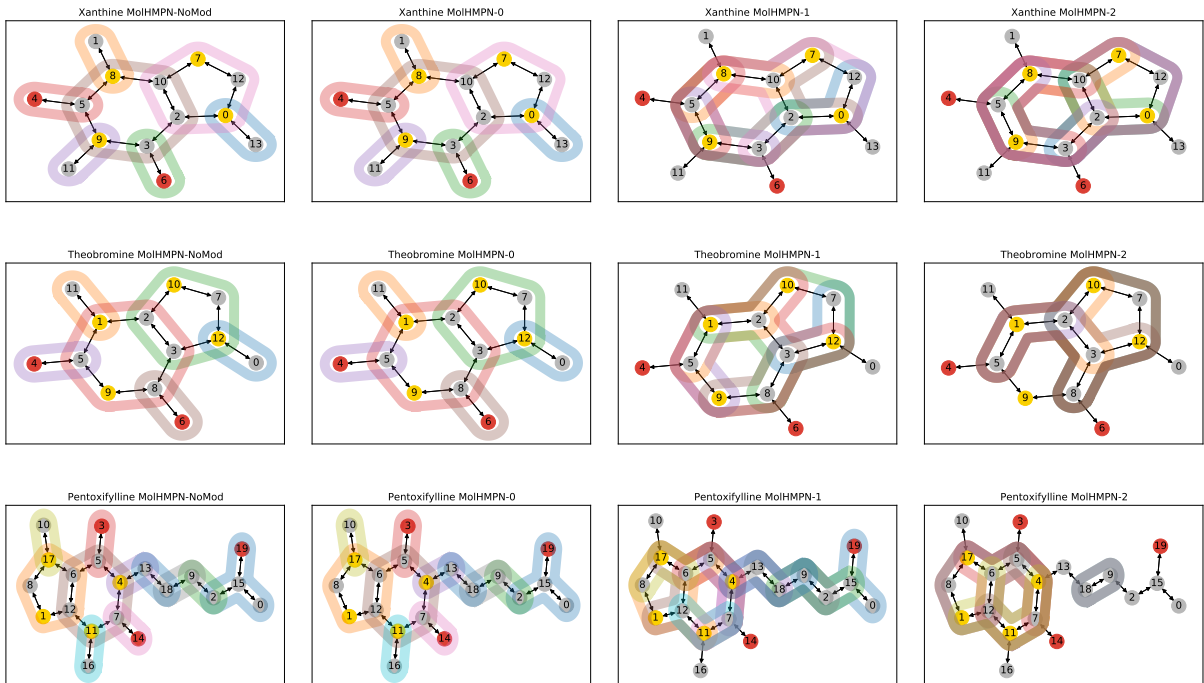


Figure 7: **Hyperedge visualization.** Comparing between the hyperedges in Mo1HMPN-NoMod and Mo1HMPN- K .

3.4 Hyperedge modification with extended hyperedges

In Section 1, we made the hypothesis that it is necessary to leverage the prior knowledge *partially* so as to overcome any potentially unsuitable prior knowledge. To test this hypothesis, we use the hyperedge extension and modification scheme. The hyperedges are extended to their K -local subgraph as stated in Section 2.1. We refer to Mo1HMPN with the K -local extension as Mo1HMPN- K , which also includes the hyperedge modification scheme. We compare Mo1HMPN- K with Mo1HMPN-NoMod, which uses the functional group hyperedges *without* the modification scheme.

Table 4: **Increasing K for hyperedge learning.** Comparison between the different K used. Results in bold are the best-performing results for their respective datasets. (\uparrow means that higher result is better and \downarrow means that lower result is better.)

Metric	AUROC (Classification)					RMSE (Regression)		
Dataset	Tox21 (\uparrow)	ClinTox (\uparrow)	SIDER (\uparrow)	BBBP (\uparrow)	BACE (\uparrow)	ESOL (\downarrow)	FreeSolv (\downarrow)	Lipophilicity (\downarrow)
Mo1HMPN-NoMod	0.839 (± 0.0147)	0.909 (± 0.0394)	0.605 (± 0.0227)	0.928 (± 0.0302)	0.892 (± 0.0232)	0.447 (± 0.0559)	0.813 (± 0.3952)	0.517 (± 0.0415)
Mo1HMPN-0	0.836 (± 0.0146)	0.903 (± 0.0392)	0.596 (± 0.0227)	0.896 (± 0.0299)	0.856 (± 0.0232)	0.454 (± 0.0339)	1.020 (± 0.3606)	0.535 (± 0.0391)
Mo1HMPN-1	0.840 (± 0.0157)	0.906 (± 0.0362)	0.605 (± 0.0124)	0.940 (± 0.0227)	0.884 (± 0.0261)	0.404 (± 0.0672)	1.090 (± 0.5495)	0.514 (± 0.1037)
Mo1HMPN-2	0.839 (± 0.0163)	0.919 (± 0.0485)	0.617 (± 0.0160)	0.905 (± 0.0298)	0.886 (± 0.0175)	0.390 (± 0.0492)	1.471 (± 0.4929)	0.619 (± 0.1104)

Table 4 shows the results of the effects of increasing K . From Table 4, we can see that the extension and modification scheme has improved the performance of Mo1HMPN-NoMod generally when $K \geq 1$. Among the datasets, FreeSolv performs significantly better in Mo1HMPN-NoMod than in Mo1HMPN- K . This is supported by the fact that FreeSolv contains fragment-like compounds where the typical size of the molecules is substantially smaller than typical small-molecule drugs [24]. Large performance degradation is observed for BBBP and Lipophilicity from Mo1HMPN-1 to Mo1HMPN-2. This may be because the extended hyperedges have deviated too far away from the original functional group design for the two datasets, and have most parts overlapped with another hyperedge, making the hyperedges indistinguishable. To have a qualitative analysis of how K affects the performances, we provide a visualization of how the hyperedge changes when K changes.

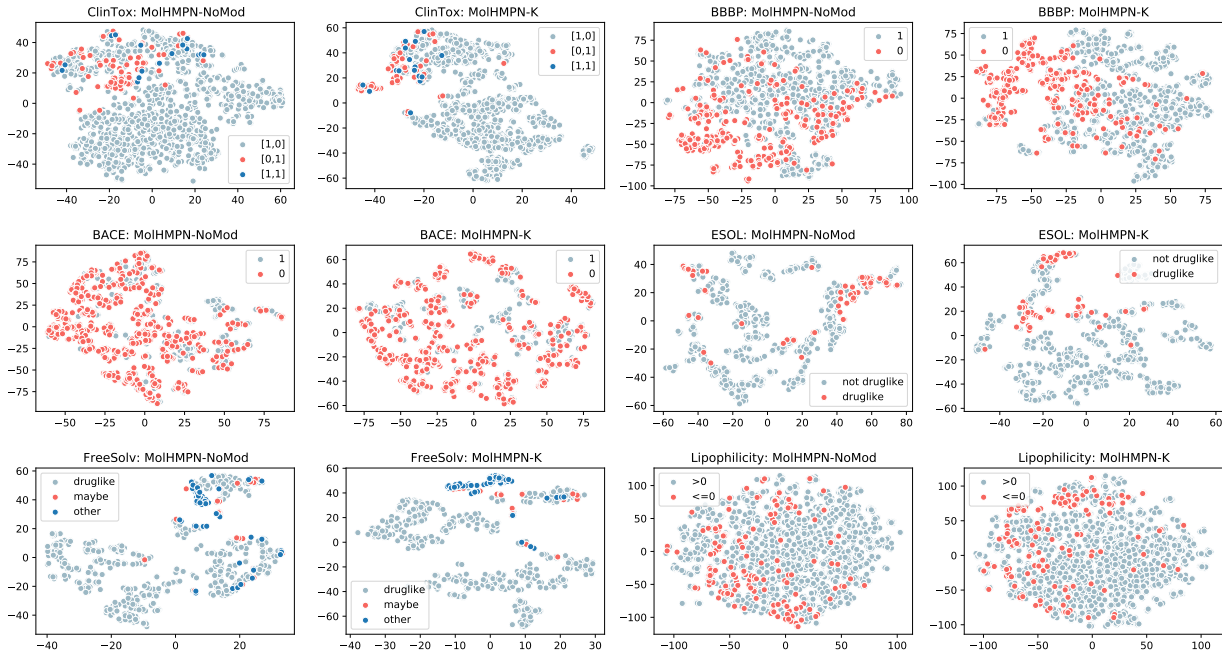


Figure 8: **t-SNE plots for MolHMPN-NoMod and MolHMPN-K.** Analyzing the contributions of the hyperedge extension and modification scheme.

We revisit xanthine, theobromine and pentoxifylline in Figure 1 to visualize the changes in the hyperedges when K changes. Figure 7 shows an example of how the hyperedges change when K changes. From Figure 7, no changes from the hyperedges were observed in MolHMPN-0 and the performance drop from MolHMPN-NoMod may be due to the difference between the MolHMPN models. When $K = 1, 2$, we can see that most parts of the purine ring (i.e. the two cyclic groups) has been covered in all three molecules, even after the hyperedge modification. The purine ring is identified as one of the most frequently-occurring substructures in drugs in the Comprehensive Medicinal Chemistry (CMC) database [5]. The substructure in pentoxifylline that is not observed in xanthine and theobromine (i.e. ketone and carbon chain) is also covered when $K = 1$. This shows that the model has captured the substructures that affects the properties of the molecules successfully.

We also provide the t-SNE plots for MolHMPN-NoMod and MolHMPN-K. Figure 8 shows the t-SNE plots for MolHMPN-NoMod and MolHMPN-K. From the BACE and Lipophilicity plots, we again do not see a clear separation between the data types. However, from the ClinTox, BBBP, ESOL and FreeSolv plots, we can see that the hyperedge extension and modification have either improved or maintained clear separability between different data types generally.

Overall, from these results, we can verify that leveraging the prior knowledge *partially* is beneficial for the molecular properties prediction.

4 Conclusion

We propose a molecular hyper-message passing network (MolHMPN) to integrate pair-wise and higher-order connectivities in molecules, and using domain knowledge-guided learnt substructures for molecular properties prediction tasks. We construct the hypergraph representation of molecules using functional groups, embed the graphs and constructed hypergraphs using the HyperMP layer, modify the membership of the hyperedges using the computed embeddings, and predict the molecular properties using the embeddings of the graphs and modified hypergraphs. We evaluate the performance of our model with several baseline methods, and show that our model is able to achieve outstanding results with only one HyperMP layer. We also analyze our design choices by comparing the results of AtomGC and FuncGC with MolHMPN-NoMod, analyze the performance of MolHMPN with increased K in hyperedge learning, and compare the performances using different types of substructures. We have verified that the incorporation of prior knowledge improves the performances and that the domain knowledge-guided hyperedge modification plays a crucial role when modeling higher-order connectivities robustly.

References

- [1] Aysha Akhtar. The flaws and human harms of animal experimentation. *Cambridge quarterly of healthcare ethics : CQ : the international journal of healthcare ethics committees*, 24:407–19, 09 2015. doi: 10.1017/S0963180115000079.
- [2] Uri Alon and Eran Yahav. On the bottleneck of graph neural networks and its practical implications. *arXiv preprint arXiv:2006.05205*, 2020.
- [3] Axel Andrés, Martí Rosés, Clara Ràfols, Elisabeth Bosch, Sonia Espinosa, Víctor Segarra, and Josep M. Huerta. Setup and validation of shake-flask procedures for the determination of partition coefficients (logd) from low drug amounts. *European Journal of Pharmaceutical Sciences*, 76:181–191, 2015. ISSN 0928-0987. doi: <https://doi.org/10.1016/j.ejps.2015.05.008>. URL <https://www.sciencedirect.com/science/article/pii/S0928098715002043>.
- [4] Song Bai, Feihu Zhang, and Philip H. S. Torr. Hypergraph convolution and hypergraph attention. *Pattern Recognit.*, 110:107637, 2021. doi: 10.1016/j.patcog.2020.107637. URL <https://doi.org/10.1016/j.patcog.2020.107637>.
- [5] Guy W. Bemis and Mark A. Murcko. The properties of known drugs. 1. molecular frameworks. *Journal of Medicinal Chemistry*, 39(15):2887–2893, 1996. doi: 10.1021/jm9602928. URL <https://doi.org/10.1021/jm9602928>. PMID: 8709122.
- [6] A.G. Blackman. *Chemistry, 4th Edition*. John Wiley & Sons, Incorporated, 2019. ISBN 9780730355038. URL <https://books.google.co.kr/books?id=AssQvwEACAAJ>.
- [7] DeepChem. Sider dataset. URL https://deepchem.readthedocs.io/en/latest/api_reference/moleculenet.html#sider-datasets.
- [8] Yifan Feng, Haoxuan You, Zizhao Zhang, Rongrong Ji, and Yue Gao. Hypergraph neural networks. *AAAI 2019*, 2018.
- [9] U.S. Food and Drug Administration. The beginnings: Laboratory and animal studies, 2015. URL <https://www.fda.gov/drugs/information-consumers-and-patients-drugs/beginnings-laboratory-and-animal-studies>.
- [10] Arup K. Ghose, Vellarkad N. Viswanadhan, and John J. Wendoloski. A knowledge-based approach in designing combinatorial or medicinal chemistry libraries for drug discovery. 1. a qualitative and quantitative characterization of known drug databases. *Journal of Combinatorial Chemistry*, 1(1):55–68, 1999. doi: 10.1021/cc9800071. URL <https://doi.org/10.1021/cc9800071>. PMID: 10746014.
- [11] Justin Gilmer, Samuel S. Schoenholz, Patrick F. Riley, Oriol Vinyals, and George E. Dahl. Neural message passing for quantum chemistry. In Doina Precup and Yee Whye Teh (eds.), *Proceedings of the 34th International Conference on Machine Learning*, volume 70 of *Proceedings of Machine Learning Research*, pp. 1263–1272. PMLR, 06–11 Aug 2017. URL <https://proceedings.mlr.press/v70/gilmer17a.html>.
- [12] Byeongho Heo, Sanghyuk Chun, Seong Joon Oh, Dongyoon Han, Sangdoo Yun, Gyuwan Kim, Youngjung Uh, and Jung-Woo Ha. AdamP: Slowing down the slowdown for momentum optimizers on scale-invariant weights. In *International Conference on Learning Representations (ICLR)*, 2021.
- [13] Sepp Hochreiter and Jürgen Schmidhuber. Long short-term memory. *Neural computation*, 9(8):1735–1780, 1997.
- [14] Kexin Huang and Marinka Zitnik. Graph meta learning via local subgraphs. In H. Larochelle, M. Ranzato, R. Hadsell, M. F. Balcan, and H. Lin (eds.), *Advances in Neural Information Processing Systems*, volume 33, pp. 5862–5874. Curran Associates, Inc., 2020. URL <https://proceedings.neurips.cc/paper/2020/file/412604be30f701b1b1e3124c252065e6-Paper.pdf>.
- [15] Andrew Jaegle, Felix Gimeno, Andrew Brock, Andrew Zisserman, Oriol Vinyals, and Joao Carreira. Perceiver: General perception with iterative attention. *arXiv preprint arXiv:2103.03206*, 2021.
- [16] Eric Jang, Shixiang Gu, and Ben Poole. Categorical reparameterization with gumbel-softmax. *arXiv preprint arXiv:1611.01144*, 2016.
- [17] Wengong Jin, Dr.Regina Barzilay, and Tommi Jaakkola. Hierarchical generation of molecular graphs using structural motifs. In Hal Daumé III and Aarti Singh (eds.), *Proceedings of the 37th International Conference on Machine Learning*, volume 119 of *Proceedings of Machine Learning Research*, pp. 4839–4848. PMLR, 13–18 Jul 2020. URL <https://proceedings.mlr.press/v119/jin20a.html>.
- [18] Masaaki Kotera, Andrew G McDonald, Sinéad Boyce, and Keith F Tipton. Functional group and substructure searching as a tool in metabolomics. *PLoS One*, 3(2):e1537, 2008.

- [19] Ruoyu Li, Sheng Wang, Feiyun Zhu, and Junzhou Huang. Adaptive graph convolutional neural networks. *CoRR*, abs/1801.03226, 2018. URL <http://arxiv.org/abs/1801.03226>.
- [20] Christopher A. Lipinski, Franco Lombardo, Beryl W. Dominy, and Paul J. Feeney. Experimental and computational approaches to estimate solubility and permeability in drug discovery and development settings. *Advanced Drug Delivery Reviews*, 23(1):3–25, 1997. ISSN 0169-409X. doi: [https://doi.org/10.1016/S0169-409X\(96\)00423-1](https://doi.org/10.1016/S0169-409X(96)00423-1). URL <https://www.sciencedirect.com/science/article/pii/S0169409X96004231>. In Vitro Models for Selection of Development Candidates.
- [21] Zichao Long, Yiping Lu, Xianzhong Ma, and Bin Dong. Pde-net: Learning pdes from data. In *International Conference on Machine Learning*, pp. 3208–3216. PMLR, 2018.
- [22] Ilya Loshchilov and Frank Hutter. Sgdr: Stochastic gradient descent with warm restarts. *arXiv preprint arXiv:1608.03983*, 2016.
- [23] MedDra. Medical dictionary for regulatory activities - meddra. URL <https://www.tga.gov.au/medical-dictionary-regulatory-activities-meddra>.
- [24] David L Mobley and J Peter Guthrie. Freesolv: a database of experimental and calculated hydration free energies, with input files. *Journal of computer-aided molecular design*, 28(7):711–720, 2014.
- [25] Junyoung Park and Jinkyoo Park. Physics-induced graph neural network: An application to wind-farm power estimation. *Energy*, 187:115883, 2019.
- [26] Maziar Raissi, Paris Perdikaris, and George E Karniadakis. Physics-informed neural networks: A deep learning framework for solving forward and inverse problems involving nonlinear partial differential equations. *Journal of Computational Physics*, 378:686–707, 2019.
- [27] Yu Rong, Wenbing Huang, Tingyang Xu, and Junzhou Huang. Dropedge: Towards deep graph convolutional networks on node classification, 2020.
- [28] Chao Shang, Jie Chen, and Jinbo Bi. Discrete graph structure learning for forecasting multiple time series. *arXiv preprint arXiv:2101.06861*, 2021.
- [29] Ying Song, Shuangjia Zheng, Zhangming Niu, Zhang-hua Fu, Yutong Lu, and Yuedong Yang. Communicative representation learning on attributed molecular graphs. In Christian Bessiere (ed.), *Proceedings of the Twenty-Ninth International Joint Conference on Artificial Intelligence, IJCAI-20*, pp. 2831–2838. International Joint Conferences on Artificial Intelligence Organization, 7 2020. doi: 10.24963/ijcai.2020/392. URL <https://doi.org/10.24963/ijcai.2020/392>. Main track.
- [30] Penghui Sun, Jingwei Qu, Xiaoqing Lyu, Haibin Ling, and Zhi Tang. Graph attribute aggregation network with progressive margin folding, 2019.
- [31] Thomas Unterthiner, Andreas Mayr, Günter Klambauer, and Sepp Hochreiter. Toxicity prediction using deep learning. *ArXiv*, abs/1503.01445, 2015.
- [32] Ashish Vaswani, Noam Shazeer, Niki Parmar, Jakob Uszkoreit, Llion Jones, Aidan N Gomez, Łukasz Kaiser, and Illia Polosukhin. Attention is all you need. In *Advances in neural information processing systems*, pp. 5998–6008, 2017.
- [33] Zhengyang Wang, Meng Liu, Youzhi Luo, Zhao Xu, Yaochen Xie, Limei Wang, Lei Cai, and Shuiwang Ji. Advanced graph and sequence neural networks for molecular property prediction and drug discovery, 2021.
- [34] Zhenqin Wu, Bharath Ramsundar, Evan N. Feinberg, Joseph Gomes, Caleb Geniesse, Aneesh S. Pappu, Karl Leswing, and Vijay Pande. Moleculenet: a benchmark for molecular machine learning. *Chem. Sci.*, 9:513–530, 2018. doi: 10.1039/C7SC02664A. URL <http://dx.doi.org/10.1039/C7SC02664A>.
- [35] Kevin Yang, Kyle Swanson, Wengong Jin, Connor Coley, Philipp Eiden, Hua Gao, Angel Guzman-Perez, Timothy Hopper, Brian Kelley, Miriam Mathea, Andrew Palmer, Volker Settels, Tommi Jaakkola, Klavs Jensen, and Regina Barzilay. Analyzing learned molecular representations for property prediction. *Journal of Chemical Information and Modeling*, 59(8):3370–3388, 2019. doi: 10.1021/acs.jcim.9b00237. URL <https://doi.org/10.1021/acs.jcim.9b00237>. PMID: 31361484.
- [36] Soojung Yang, Doyeong Hwang, Seul Lee, Seongok Ryu, and Sung Ju Hwang. Hit and lead discovery with explorative rl and fragment-based molecule generation, 2021.
- [37] Ayesha Zafar and Jóhannes Reynisson. Hydration free energy as a molecular descriptor in drug design: A feasibility study. *Molecular Informatics*, 35, 04 2016. doi: 10.1002/minf.201501035.

A Appendix

A.1 Hypergraph construction

In this section, we provide the list of functional groups that have been utilized in our current study based on their central atoms. We highlight the central atoms and their respective first- and second-hop neighbors with circles of different colors.

Table A.1: **Functional groups with nitrogen as the central atom.** The red circles represent the central atoms, and the blue and green circles represent the 1-hop and 2-hop neighbors from the central atom respectively.

Functional group	Structure	Hyperedge	Functional group	Structure	Hyperedge
Amine			Nitro		
Nitrate			C nitroso		
N nitroso			Azo		
Hydrazine			Hydroxylamine		
Nitrile					

Table A.2: **Functional groups with carbon as the central atom.** The red circles represent the central atoms, and the blue and green circles represent the 1-hop and 2-hop neighbors from the central atom respectively.

Functional group	Structure	Hyperedge	Functional group	Structure	Hyperedge
Alkene			Alkyne		
Aldehyde			Ketene		
Isocyanate			Carboxyl		
Carbamate			Carbamide		
Amide			Ketone		
Isothiocyanate			Thione		
Thioamide			Thiourea		
Carbodiimide			Carboximidamide		
Imine			Hydrazone		
Oxime			Alcohol		
Thiol			Allene		

Table A.3: **Functional groups with oxygen as the central atom.** The red circles represent the central atoms, and the blue and green circles represent the 1-hop and 2-hop neighbors from the central atom respectively.

Functional group	Structure	Hyperedge	Functional group	Structure	Hyperedge
Ether			Peroxide		

Table A.4: **Functional groups with phosphorus as the central atom.** The red circles represent the central atoms, and the blue and green circles represent the 1-hop and 2-hop neighbors from the central atom respectively.

Functional group	Structure	Hyperedge	Functional group	Structure	Hyperedge
Phosphanyl			Phosphine oxide		
Phosphite ester			Phosphodiester		

Table A.5: **Functional groups with sulfur as the central atom.** The red circles represent the central atoms, and the blue and green circles represent the 1-hop and 2-hop neighbors from the central atom respectively.

Functional group	Structure	Hyperedge	Functional group	Structure	Hyperedge
Disulfide			Sulfoxide		
Sulfone			Sulfonamide		
Sulfonate			Thioether		
Sulfate					

A.2 Training details

In this section, we provide the data and training details.

Data details. The tasks that are carried out includes five classification (Tox21, ClinTox, SIDER, BBBP and BACE) and three regression (ESOL, FreeSolv and Lipophilicity) tasks. The dataset descriptions are given as follows:

- The Toxicology in the 21st Century (Tox21) [34, 31] dataset was created to assess the potential of drugs to disrupt biological pathways that may result in toxicity. It contains 8014 compounds with 12 different targets, which include the nuclear receptor (NR) and stress response (SR) pathways. NRs are one of the essential classes of transcriptional factors that play a critical role in human development, metabolism and physiology. The inappropriate activation of NRs can lead to a broad spectrum of negative health effects. SR pathways are the cellular and organismal mechanisms that resist the effects of cellular stress, which can lead to apoptosis.
- The ClinTox dataset compares the drugs that are approved by the FDA and drugs that have failed the clinical tests [34]. It contains 1491 drug compounds with 2 tasks: the clinical trial toxicity and the FDA approval status.
- The Side Effect Resource (SIDER) [7] dataset contains information on marketed medicines and their adverse drug reactions. It contains 1427 approved drugs with 27 tasks that are grouped based on their side effects on 27 system organ classes following the MedDRA classifications [23].
- The Blood-brain barrier penetration (BBBP) dataset was created to model and predict the barrier permeability. It contains over 2000 compounds with 1 task that evaluates the permeability of the compounds. The Blood-Brain Barrier separates the circulating blood and the brain extracellular fluid, and protects the brain from foreign substances in the blood that may damage the brain. Hence, BBBP is one of the key factors in chemical toxicological studies and in drug design.
- The Beta-Secretase 1 (BACE) dataset consists of small molecule inhibitors, and provides quantitative IC50 and qualitative binding results for a set of inhibitors of human beta-secretase 1 (BACE1). The BACE dataset contains 1522 compounds with 1 task that provides the binding results for the inhibitors. BACE is essential for the production of the toxic amyloid beta that is critical in early part in the Alzheimer’s disease pathogenesis.
- The Estimated Solubility (ESOL) dataset contains information on the water solubility of compounds. The ESOL dataset has 1128 compounds. The knowledge of thermodynamic solubility of drug candidates is important in drug discover as it is related to the drug absorption in the body [20].
- The Free Solvation Database (FreeSolv) provides the calculated hydration free energy of fragment-like compounds in the water and provides a test of potential relevance to the binding affinity calculations for drug discovery [34]. FreeSolv contains 643 compounds.
- The Lipophilicity dataset [33] was used for the prediction of octanol/water distribution coefficient (logD at pH 7.4). It contains 4200 compounds. The lipophilicity of drug molecules affects both the membrane permeability and solubility.

We use the AtomFeaturizer and BaseBondFeaturizer of DGL-LifeSci to extract the features from the initial atom and bond features. The hypergraphs are constructed using DGL and Networkx. The dataset information are given in Tables A.6, A.7 and A.8.

Table A.6: Datasets types, number of tasks, performance metric and split type

Dataset	Task	Number of tasks	Metric	Split
Tox21	Classification	12	AUROC	Random
ClinTox	Classification	2	AUROC	Random
SIDER	Classification	27	AUROC	Random
BBBP	Classification	1	AUROC	Random
BACE	Classification	1	AUROC	Random
ESOL	Regression	1	RMSE	Random
FreeSolv	Regression	1	RMSE	Random
Lipophilicity	Regression	1	RMSE	Random

Table A.7: Atom features used to featurize the node features

Atom Features	Number of Features
atom type one hot	43
atomic number	1
atom mass	1
atom degree one hot	11
atom explicit valence one hot	6
atom implicit valence one hot	7
atom total num H one hot	5
atom formal charge one hot	5
atom hybridisation one hot	5
atom num radical electrons one hot	5
atom is aromatic one hot	2
atom is in ring one hot	2
atom chiral tag one hot	4
atom chirality type one hot	2
atom is chiral center	1

Table A.8: Bond features used to featurize the edge features

Bond Features	Number of Features
bond type one hot	4
bond is in ring	1
bond is conjugated one hot	2

The training details can be found in Table A.9 and A.10.

Table A.9: Hyperparameters for MolHMPN-NoMod

Dataset	x_k	Cycles	GNN dropout	Regressor dropout	MLP neurons	Latent dimensions
Tox21	ZERO	FALSE	0.2	0.2	[64]	128
ClinTox	ZERO	FALSE	0.3	0.3	[64, 32]	128
SIDER	MEAN	FALSE	0.0	0.1	[64]	128
BBBP	MEAN	FALSE	0.0	0.0	[128]	256
BACE	MEAN	TRUE	0.2	0.0	[64, 32]	128
ESOL	MEAN	TRUE	0.0	0.0	[128]	256
FreeSolv	MEAN	FALSE	0.4	0.4	—	128
Lipophilicity	MEAN	FALSE	0.2	0.2	—	128

Table A.10: Hyperparameters for MolSoft and MolHMPN-0,1,2,3

Dataset	x_k	Cycles	GNN dropout	Theta dropout	Regressor dropout	MLP neurons	Latent dimensions
Tox21	ZERO	FALSE	0.2	0.2	0.2	[64]	128
ClinTox	ZERO	FALSE	0.3	0.3	0.3	[128]	256
SIDER	MEAN	FALSE	0.0	0.0	0.1	[64]	128
BBBP	MEAN	FALSE	0.0	0.0	0.0	[128, 64]	256
BACE	MEAN	TRUE	0.0	0.0	0.0	[128]	256
ESOL	MEAN	TRUE	0.0	0.0	0.0	[128]	256
FreeSolv	MEAN	FALSE	0.4	0.4	0.4	—	128
Lipophilicity	MEAN	FALSE	0.2	0.2	0.2	—	128

In this section, we provide the details of the hyperedge construction of MolSoft.

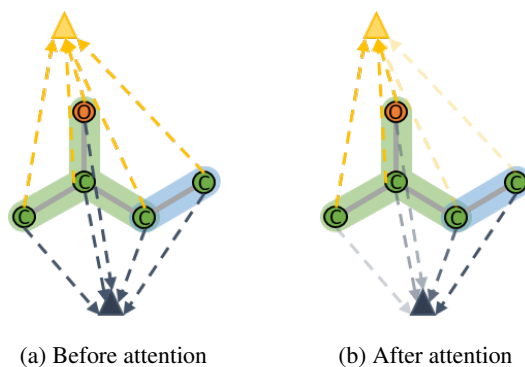


Figure A.1: **MolSoft hypergraph construction.** The green and blue shaded parts in the molecule are the hyperedges defined in MolHMPN-NoMod. We set the number of hyperedges in MolSoft to be the same as that in MolHMPN-NoMod. To let the model learn the substructures, we assign all nodes in a molecule to each hyperedge as shown in a), where each dashed-arrow represents the edge that connects each node to each hyperedge. After the attention mechanism has been employed, the edges that connects the nodes to hyperedges are reweighed as shown in b).